


Dynamic Experiments using Simultaneous Compression and Shear Loading

B. Claus¹  · J. Chu¹ · M. Beason² · H. Liao¹ · B. Martin³ · W. Chen¹

Received: 14 March 2017 / Accepted: 30 June 2017 / Published online: 10 July 2017
© Society for Experimental Mechanics 2017

Abstract Material characterization at high strain rates under simultaneous compression and shear loading has been a challenge due to the differing normal and shear wave speeds. An experimental technique utilizing the compression Kolsky bar apparatus was developed to apply dynamic compression and shear loading on a specimen nearly simultaneously. Synchronization between the compression and shear loading was realized by generating the torsion wave near the specimen which minimizes the time difference between the arrival of the compression and torsion waves. This modified Kolsky bar makes it possible to characterize the dynamic response of a material to combined

compression and shear impact loading. This method can also be applied to study dynamic friction behavior across an interface under controlled loading conditions. The feasibility of this method is demonstrated in the dynamic characterization of a simulant polymer bonded explosive material.

Keywords Simultaneous torsion and compression · Kolsky bar · Split Hopkinson pressure bar · Friction · Shear

Introduction

Traditionally, experiments are conducted in one of the simple stress states: tension, compression, torsion, or flexure. Many material properties such as Young's modulus, shear modulus, yield strength, and rupture modulus are obtained for these simple stress states. Complicated stress states are typically simplified using material models, which often treat materials as continuous, homogeneous, and isotropic in order to establish an equivalent simple stress state from more complicated ones. However, many materials are intrinsically anisotropic and are also subjected to multiaxial dynamic loading, making it necessary to characterize these materials under realistic strain rates and multi-axial stress states. Two examples are damaged armor materials subjected to impact by pointed projectiles; and dynamic friction which calls for simultaneous normal pressure and shear loading.

Material properties at high strain rates are typically characterized using the Kolsky bar (the split Hopkinson pressure bar), the advent of which marked a new era of material characterization by enabling the study of materials at strain rates between 100/s and 10,000/s [1, 2]. This apparatus has been developed and implemented to study tensile, compressive, torsional, and flexural properties of many materials.

✉ B. Claus
bclaus@purdue.edu

J. Chu
chu82@purdue.edu

M. Beason
mbeason@purdue.edu

H. Liao
liao23@purdue.edu

B. Martin
bradley.martin.11@us.af.mil

W. Chen
wchen@purdue.edu

¹ Purdue University, 701 W. Stadium Ave,
West Lafayette, IN 47907, USA

² Purdue University, 500 Allison Road,
West Lafayette, IN 47907, USA

³ U.S. Air Force Research Laboratory,
101 W. Eglin Blvd. Suite 135,
Eglin AFB, FL 32542, USA



The Kolsky bar has even been used to study materials in states of triaxial pressure, a particularly useful technique for geomaterials [3, 4].

Of the three types of Kolsky bar, the compression Kolsky bar provides a simple, yet versatile means to characterize the compressive behavior of materials [1, 2]. With pulse shaping [3, 5] and single loading techniques [6], materials ranging from soft, porous foams to brittle ceramics may be studied *in situ* and *ex post facto* to reveal the damage processes as well as material behavior on the microscopic scale.

Traditionally, torsion experiments are conducted using a stored torque torsion Kolsky bar. This variant of the torsion Kolsky bar utilizes a strategically placed clamp to control the duration of the torsional wave while the amplitude is determined simply by the amount of torque stored prior to the experiment [7–9]. Torsion waves have also been generated via transverse loading through explosives, and deformable tubing was used to produce torsional waves with a desired shape [5]. For more control over the duration and profile of the incident torsion wave, the side-impact torsion Kolsky bar was developed [10, 11]. However, for experiments involving multiple stress states (such as friction), an additional form of loading must be incorporated into the experiment [8–10, 12].

Loading a specimen with multiple stress states in a controlled manner has proven to be non-trivial. Dynamic experiments are a prime example of this condition, particularly in the manner regarding wave propagation since each mode of loading may experience different wave speeds (bulk, longitudinal, shear, etc.). For the Kolsky bar experiment, differing wave speeds pose a particularly challenging timing issue that must be resolved with micro-second accuracy [13–15]. Many approaches have been developed to avoid this particular timing issue.

One approach is to use a typical compression bar, except with a rotating transmission bar [12]. Upon arrival of the incident compression wave, the specimen engages with the rotating transmission bar to provide dynamic compressive and torsional stresses. This clever method can supply a near constant shearing rate, but the rate is not directly proportional to the incident compression loading. A technique using a compression Kolsky bar relies on an inclined plane to partially convert an axial compression wave into a transverse shear wave [16, 17]. A similar technique using a modified compression Kolsky bar relies on a wedge to transmit compression and shear into two transmission bars, enabling the study of both friction and combined compression-shear loading on a single or pair of materials [18, 19]. However, with these techniques, the shear stress is not necessarily evenly distributed over the contact area.

To achieve rate constancy in experiments involving multiaxial stress, and to gain control over the normal and shear

loading, a new robust method is desired. Through modification of the compression Kolsky bar, the dynamic behavior of materials subjected to combined simultaneous compression and shear loading may be characterized. A new modification to the compression Kolsky bar is presented that realizes nearly simultaneous normal and torsion stress wave loading on the specimen.

Materials and Methods

The experiment is based upon a modified compression Kolsky bar. Modifications to the compression Kolsky bar result in the production of torsional stresses within the bar in addition to compressive stresses which load the specimen. In principle, the normal and shear quantities can be calculated using the one dimensional wave equations for compression and torsion in a decoupled state (equations (1) and (2)), with $\Delta\sigma$ and $\Delta\tau$ the change in normal and shear stress, ρ the bar density, C_L and C_S the longitudinal and shear wave speeds, r the bar radius, and Δv and $\Delta\dot{\phi}$ the longitudinal and angular particle velocities.

$$\Delta\sigma = \rho C_L \Delta v \quad (1)$$

$$\Delta\tau = \rho C_S r \Delta\dot{\phi} \quad (2)$$

Modified Kolsky Bar

When the specimen is a very soft material or the transmitted signal is expected to be very small, the conventional incident-transmission bar configuration of the Kolsky bar experiment must be changed. For example, a very soft specimen results in a weak transmitted stress that is not easily measured. Similarly for friction experiments, a small friction coefficient could also lead to a weak transmitted stress. Since stress and particle velocity are directly related in the Kolsky bar experiment (equation (1)), this implies that the transmitted particle velocity is near zero and that the transmission bar may be replaced by a sufficiently rigid force transducer. This same assumption holds true in tension, compression, and torsion. The apparatus has been designed as a modified form of the compression Kolsky bar without a transmission bar (Fig. 1). Although, this assumption is not a requirement for the simultaneous compression-shear technique, where sufficiently strong or rigid materials may permit the use of a transmission bar.

The apparatus contains all of the features of a compression Kolsky bar with barrel, striker, pulse shaper, flange and single loading device [6], and incident bar. The modifications come into place near the specimen. Since the experiments are to involve compression and torsion, loads



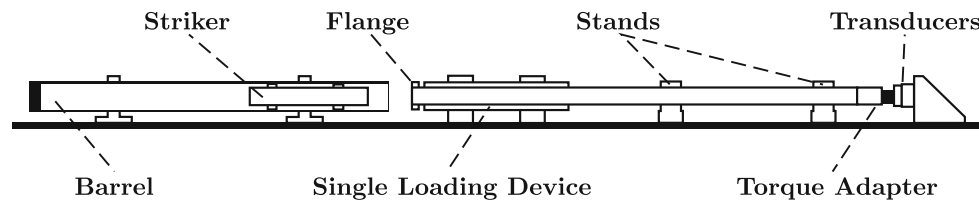


Fig. 1 The modified compression Kolsky bar with both force and torque transducers instead of a transmission bar. The barrel, striker, single loading device, and incident bar are identical to that of a typical compression bar. The primary difference is the torque adapter which is mated to the incident bar via a key-slot joint

are measured via a force transducer and a torque transducer. The loads are applied through a torque adapter, of which the geometry can be tailored towards a target stress state (Fig. 2). However, care should be taken when selecting force and torque transducers, as size and mass can induce time delays and inertial effects in the measured force and torque. Also, if dual mode transducers (i.e. force-torque transducers) are not being employed and fairly strong materials are being studied, care should be taken to account for errors in the load measurements when the transducers are exposed to eccentric loads (i.e. shear on an axial force transducer or axial force on a torque transducer). If the materials being studied are soft, then the axial and torsional loads will most likely be small and measurement errors would be negligible.

Following insights from the design of the side-impact torsion Kolsky bar [10], the specimen end of the compression bar was modified with a key-slot design in order to provide a simple coupling that would also transmit torque (Fig. 2(a)). A two-piece adapter composed of a mating screw surface and the opposing end of the key-slot provides the means to produce the torsional wave upon loading from the incident compression wave (Fig. 2(b)).

The design of the bar differs from those in literature by the fact that both modes, compression and torsion, are

generated using a solitary mechanism. However, the production of a torsional stress within the specimen, and the rates (both axial and angular) at which the specimen is loaded are fixed proportionally to the pitch of the screw. The physical specimen and the second half of the pitched adapter become a virtual specimen (Fig. 2(c)). The pitch angle controls the ratio of shear stress to compressive stress.

In an ideal experiment, the incident compression wave would encounter the pitched interface just prior to the sample and deliver a combined loading of compression and torsion to the specimen. At this time, the motion of an adapter with identical material as that of the incident bar is better described in terms of velocity. To investigate this matter, three cases should be considered.

The first and most trivial case is where the adapter is not allowed to rotate. In this case, neglecting the wave impedance of the interface, the adapter would be expected to move forward and separate from the incident bar at the striking velocity.

The second case is just the opposite of the first, where the axial velocity is fixed at zero, but the adapter is permitted to rotate. In this case, the end of the incident bar would be expected to move forward at the same speed as with typical Kolsky bar data reduction. In other words, from the one dimensional longitudinal wave equation, the particle velocity in the bar just prior to the pitched surfaces is described by the sum of the measured incident (σ_I) and reflected compression (σ_R) waves, the bar density (ρ_B), and the bar wave speed (C_B) (equation (3)). The adapter would then be forced to rotate at an angular velocity (ω_A) proportional to the pitch (p_A , in revolutions per unit length) of the inclined planes (equation (4)).

$$v_{Bar\,End} = \frac{\sigma_I - \sigma_R}{\rho_B C_B} \quad (3)$$

$$\omega_A = v_{Bar\,End} \cdot p_A \quad (4)$$

The issue of the inclined plane is critical to the operation of the apparatus. In the sense related to Kolsky bar experiments, the interface between the torque adapter must be well defined and with sufficiently tight tolerances such that all portions of the incident wave will interact with the

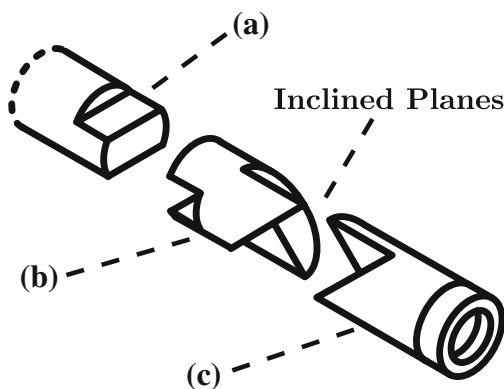


Fig. 2 The torque adapter is mated to the incident bar with a key-slot joint (a) [10]. The first half of the adapter (b) has the mating side of the key-slot joint and torque generating geometry (two inclined planes in this case) The second part of the adapter (c) has another set of torque generating geometry and a flat end for mounting the specimen

torque adapter. The trade off for manufacturability comes at a cost of increased mathematics. Since a double helix with relatively low pitch is fairly difficult to machine, a pair of inclined planes may provide a suitable substitute.

The third case is the most non-trivial, involving both axial and angular velocities. Considering the assumption that the specimen has very low wave impedance, the amount of torque required to rotate the adapter would be small and potentially unmeasurable, hence the use of force and torque transducers. However, this assumption is particularly tailored to friction experiments and might not be necessary for shear experiments involving hard materials.

Adapter Geometry

The specimen is loaded nearly simultaneously with compression and torsion through the use of the torque adapter, a two-piece mechanism that connects the specimen to the incident bar. The geometry of the adapter plays an important role in determining how much torque is applied to the specimen. The most convenient choice would be a double helix with a low pitch. However, this type of geometry, while fairly easy to explain, is also more difficult to machine to the necessary tolerances required for wave propagation. A much simpler alternative is a pair of inclined planes (Fig. 2).

With a circular cross section, the inclined plane is easily parameterized (Fig. 3 and equation (5)) in polar coordinates in terms of the bar radius (R_B), the polar angle (ϕ), and the angle of incline (θ). Since the contact point between two similar parts will be on the outer edge of the inclined surface, the components of the incoming axial motion will be transmitted according to the tangent vector which is

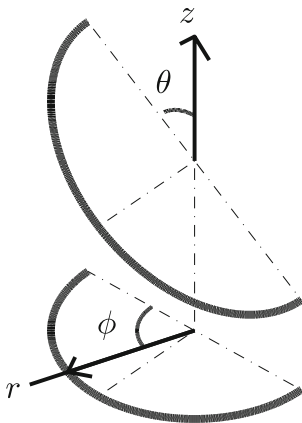


Fig. 3 Projection of the circular bar cross-section onto the inclined plane at angle θ . The coordinate system is polar (r, z, ϕ), with the z axis aligned with the bar axis

found through the derivative with respect to the polar angle (equations (6) and (7)).

$$\mathbf{p} = R_B \begin{Bmatrix} 1 \\ \cos(\phi) \cos(\theta) \\ \phi \end{Bmatrix} \quad (5)$$

$$\mathbf{p}_t = R_B \begin{Bmatrix} 0 \\ -\sin(\phi) \cos(\theta) \\ 1 \end{Bmatrix} \quad (6)$$

$$\mathbf{p}_t = \frac{1}{\sqrt{1 + \sin^2(\phi) \cos^2(\theta)}} \begin{Bmatrix} 0 \\ -\sin(\phi) \cos(\theta) \\ 1 \end{Bmatrix} \quad (7)$$

When the two parts of the adapter are closed (the relative angle is zero), the inclined planes are fully in contact. This condition would lead to full transmission of the compressive load and no production of torque. When the adapters have a non-zero relative angle (ϕ_0), the contact point shifts by an amount equal to the half angle from the midpoint of the arc (at $\pi/2$). In other words, since the adapter is a pair of mating surfaces, the effective rotation of one part is described by half of the initial angle. Through a trigonometric identity (equation (8)), the tangent vector can then be represented in terms of the relative angle (equation (9)), providing the coefficients necessary for determining the amount of torque produced from a given compressive load.

$$\sin\left(\frac{\pi}{2} - \frac{\phi_0}{2}\right) = \cos\left(\frac{\phi_0}{2}\right) \quad (8)$$

$$\mathbf{p}_t = \frac{1}{|\mathbf{t}|} \begin{Bmatrix} 0 \\ -\cos\left(\frac{\phi_0}{2}\right) \cos(\theta) \\ 1 \end{Bmatrix} \quad (9)$$

Measurements and Data Reduction

For a system with an incident bar and transmission bar, two sets of strain gages (one half-bridge for compression and one full-bridge for torsion) would be required for each bar. However, with the assumption that the specimen has very small wave impedance, measurements may only be made with one set of strain gages in a half-bridge configuration for compression, a force transducer, and a torque sensor. For a specimen with small wave impedance, the torsional stress produced in the incident bar by the adapter is not of sufficient magnitude to be measured accurately.

For clarification, there are four assumptions necessary for reducing the data from experiments conducted on the modified Kolsky bar:

1. The force transducers represent a fixed boundary with zero particle velocity.

2. The incident bar maintains an angular velocity of zero for all time.
3. The torque adapter has a sufficient initial angle such that closure does not occur during the experiment.
4. The torque adapter does not separate during the experiment.

The second assumption implies that as the incident bar moves forward, the torque adapter will itself rotate and the bar will not. So long as the torque adapter has a resistive torque, whether through friction or material response of the specimen, there should not be any loss of contact between the torque adapter and the incident bar and the fourth assumption will be satisfied.

Knowing the geometry of the specimen, the measured force and torque can be reduced into the compression and shear stresses of the specimen. Regardless of shape, the compressive stress (σ_S) can be found using only the measured force (F_S) and the cross-sectional area (A_S) (equation (10)). The shear stress (τ_S) depends upon the measured torque (T_S) and the geometry specific for each type of experiment. If the specimen is the shape of a disc, equation (11) may be used to determine the shear stress with the disc radius (r_S) and the torsion constant (J_S). However, if the specimen is an annulus with the inner radius (r_i) and the outer radius (r_o), equation (12) is preferred. For friction experiments, the friction coefficient (μ) is then calculated using the Coulomb friction law (equation (13)).

$$\sigma_S = \frac{F_S}{A_S} \quad (10)$$

$$\tau_S = \frac{T_S \cdot r_S}{J_S} \quad (11)$$

$$\tau_S = \frac{2}{3} \frac{(r_o^2 + r_o r_i + r_i^2) T_S}{(r_o + r_i) J_S} \quad (12)$$

$$\mu = \frac{\tau_S}{\sigma_S} \quad (13)$$

To determine the motion of the torque adapter, the measured stress in the bar must first be converted to velocity (equation (1)). Since the adapter may only move at the same speed or faster than the incident bar, the motion of the adapter is easily determined using velocities. The velocity of the end of the incident bar (v_{BE}) is determined by the incident and reflected stresses (σ_I and σ_R) through the density (ρ) and elastic bar wave speed (C_B) of the incident bar (equation (3)).

The motion of the torque adapter may then be determined through the tangent vector of the elliptical boundary of the inclined plane (equation (9)), producing the axial

(v_{AA}) and transverse (v_{AT}) particle velocities of the adapter (equation (14) and (15)).

$$v_{AA} = \frac{R \cdot v_{BE} \cdot \cos\left(\frac{\phi_0}{2}\right) \cos(\theta)}{\sqrt{1 + \cos^2\left(\frac{\phi_0}{2}\right) \cos^2(\theta)}} \quad (14)$$

$$v_{AT} = \frac{v_{BE}}{\sqrt{1 + \cos^2\left(\frac{\phi_0}{2}\right) \cos^2(\theta)}} \quad (15)$$

The angular velocity ($\dot{\phi}_A$) of the adapter may be found through (equation (16)) through division by the bar radius (R_B). Further quantities related to the particular experiment may be determined using conventional data reduction techniques. For example, in a compression-shear experiment, the axial strain rate ($\dot{\epsilon}$) and shear strain ($\dot{\gamma}$) rate would be determined through the length of the specimen (L_S) (equations (17) and (18)). In a friction experiment, the axial strain rate would still be determined by equation (17), but the angular velocity of the adapter would then become the sliding velocity (v_{ST}) as in equation (19).

$$\dot{\phi}_A = \frac{v_{AT}}{R_B} \quad (16)$$

$$\dot{\epsilon} = \frac{v_{AA}}{L_S} \quad (17)$$

$$\dot{\gamma} = \frac{v_{AT}}{L_S} \quad (18)$$

$$v_{ST} = \frac{2}{3} \frac{(r_o^2 + r_o r_i + r_i^2) v_{AT}}{(r_o + r_i) R_B} \quad (19)$$

With the angular velocity of the adapter ($\dot{\phi}_A$), the assumption that the adapter does not close can be checked through integration (equation (20)). The progression of this angle is also effectively limited by the use of a single loading device which limits the forward motion of the incident bar [6].

$$\phi_0 - \int \dot{\phi}_A dt > 0 \quad (20)$$

Kolsky Bar Apparatus

The modified Kolsky bar apparatus used in these experiments was precision ground to 12.7 mm in diameter from Aluminum 7075-T6 stock. The striker was machine to be 280 mm in length and the incident bar to be 1.67 m in length. The incident bar also had two flats machined on the specimen end to a depth of 6 mm. The flange on the impact end of the incident bar was machined from 4140 steel and threaded onto the incident bar with 1/2-20 threads. The threads were sealed with PTFE thread tape to reduce interference with the incident stress wave. The axial strain in the incident bar



was measured with a half Wheatstone bridge and the shear strains with a full Wheatstone bridge. The axial force on the specimen was measured with a Kistler quartz force transducer, and similarly for the torque acting on the specimen. The torque adapters were mated to the incident bar with a matching 6 mm deep slot, multiple adapters were machined with various inclination angles (45, 60, and 75 degrees). In addition, a sleeve bearing was used to support the torque adapters in order to maintain alignment with the incident bar.

Specimen Geometry

Due to the assumption that the specimen has relatively low wave impedance compared to the incident bar, materials are limited to small size, or low longitudinal and shear moduli. Favoring the latter, many materials are still suitable for study with the modified Kolsky bar apparatus. These include, but are not limited to foams, rubbers, soft composites, and other porous media.

Depending on the material, the specimen could be one of two shapes: a right circular cylinder with outer radius (r_o) and length (L_s); or an annulus with inner radius (r_i), outer radius (r_o) and length (L_s) (Fig. 4). Of the two, the annulus is favored for torsion experiments because the variables of interest can be defined over a finite area with minor variations about the mean [8, 9]. However, the annulus is the more complicated of the two shapes to fabricate, particularly for soft materials. Fortunately, some materials such as energetics and their simulants can be cast into shape and processed at a later time.

Specimen Preparation

The material used in this study was a PBXn-301 simulant composed of 80% aggregate and 20% binder cast into tubular raw material (Fig. 5). The mold was constructed from three drill bushing and a dowel rod, components that are

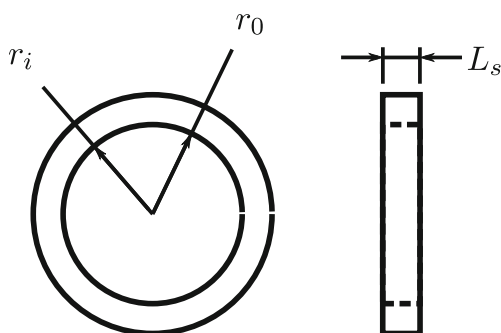


Fig. 4 An annular specimen with inner radius (r_i), outer radius (r_o), and thickness (L_s). An annular specimen is all but required for studying friction using a torsion Kolsky bar

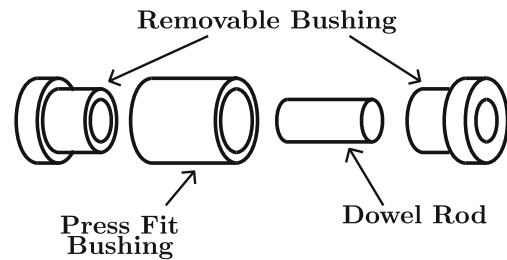


Fig. 5 A four piece mold comprised of three drill bushings and a dowel rod. Internal surfaces were ground to prevent the cast material from adhering to the inside. The mold produces a tube which can later be cut into thin annular specimens

commercially available with tight tolerances. Each component of the mold was then ground and polished to prevent the cast material from sticking inside the mold. A mold release agent was not used because of the tendency of the aggregate to absorb liquids.

Once the simulant was cured, the tube was extruded from the mold and sliced into thin sections. Each specimen was then placed in an external support structure (a Teflon™ bushing) and ground for flatness. The finished annuli (Fig. 4) had an outer diameter of 12.7 mm, an inner diameter of 9.5 mm, (providing a wall thickness of 1.6 mm), and a thickness (or length) of 1.6 mm.

The samples were then adhered to their own torque adapter. The torque adapter was then installed on the hybrid Kolsky bar with the desired initial angle (Fig. 6) and adhered to a platen fixed to the load transducers. In the case of friction experiments, the last step was neglected with the intention of studying friction between the specimen and the platen.

Results

The major benefit of using a compression Kolsky bar to deliver combined compression and torsion is the simplicity of the apparatus. The compression technique is mature and well developed with respect to repeatability and reliably controlling the profile of the incident waveform.

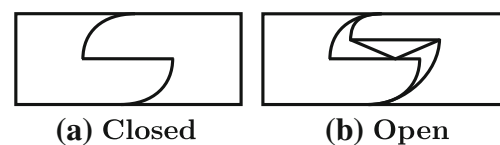


Fig. 6 The torque adapter in the (a) closed position and (b) open position. The adapter does not produce torque in the closed position. The contact points depend on whether the mating surfaces are inclined planes, a true screw, or a double helix

Initial experiments with the various torque adapters (with inclination angles of 45, 60, and 75 degrees) and soft specimen materials proved that the shear stresses produced in the incident bar were too small to be measured accurately. This ultimately changed the course of the data reduction procedure and required validation of the motion of the torque adapter through optical techniques (see the Discussion section for more details on this matter). Typical incident and reflected signals are shown in Fig. 7.

Dynamic Friction

The experiments involving friction were conducted with identical conditions: a striking velocity of 4.5 meters per second, a copper pulse shaper (6 mm in diameter and 1.1 mm thick), and a gap in the single loading device of 0.5 mm. The gap in the single loading device was chosen such that only the first incident wave would load the specimen, after reflection back at the striking end of the bar, the single loading device would be “closed” and motion of the incident bar would effectively be reversed, thus preventing further loading of the specimen.

Due to the nature of the friction experiment, the second piece of the torque adapter (Fig. 2(c)), and the specimen are free floating. In order to prevent misalignment and ejection of the torque adapter, it was necessary to maintain alignment with the use of a sleeve bearing. The side of the sleeve bearing also had to be removed (i.e. an open-sided sleeve bearing) such that the initial angle of the torque adapter could be set and checked before each experiment.

Since this technique involves dynamic compression, if the initial stress state is trivial (there is no stress), then friction measurements will not make sense due to the inverse relationship in the Coulomb friction law (equation (13) and

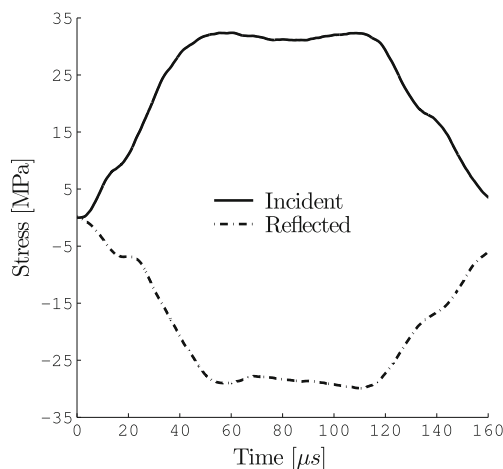


Fig. 7 Typical incident and reflected signals measured from the incident bar. The low wave impedance of the specimen results in very little change in the reflected signal from the incident signal

Fig. 8(a)). However, the results will become more relevant as the compressive load increases to a non-zero value (Fig. 8(d)).

The dynamics of the system produce interesting strain rate and compression results (Fig. 8(c) and (d)). As the angle of inclination is increased, the angular velocity (and hence the sliding velocity) of the torque adapter must also increase in order for the torque adapter to conform to the motion of the incident bar (Fig. 8(b)). As such, it is expected that the torque adapter would exert a greater axial force on the specimen. This increase in the force would also imply that a specimen would experience a greater axial strain rate as well. However, since momentum must be conserved, and the angular velocity has been increased, the axial velocity must show a decrease, resulting in a lower axial strain rate.

Dynamic Shear

The shear experiments were conducted with the same striking velocity of 4.5 meters per second as the friction experiments. The single loading device was also set with a gap of 0.5 mm, but the copper pulse shaper was 7.1 mm in diameter and 0.5 mm thick. Unlike the friction experiment, the specimen was adhered to both the torque adapter and force transducer. However, the sleeve bearing was still used to guarantee alignment of the torque adapter.

The axial strain rate and stress follow the same trend as in the friction experiments (Fig. 9(a) and (b)). As the inclination angle is increased, the axial strain rate decreases, but the axial force increases. The shear response of the specimen provides some insight into the friction experiments as well. Since the specimen was adhered to the transducer assembly, the material response of the specimen plays a greater role in the dynamics of the system, ultimately reducing the effectiveness of the various torque adapters in changing the shear strain rate (Fig. 9(c)). Since the motion of the torque adapter is driven by the incident bar, and that motion was restricted to be consistent across all of the experiments, the shear stress-strain curves extend out to the same shear strain (Fig. 9(d)).

Discussion

The compression Kolsky bar modified for simultaneous compression and torsion provides a new set advantages and disadvantages for characterizing the dynamic behavior of materials. The advantages are that the compression-shear response of materials can be measured and quantified; and friction can be measured in dually dynamic states.

Some disadvantages are inherited from the compression Kolsky bar itself, primarily in that the total strain is driven by the duration of the incident signal (which is determined

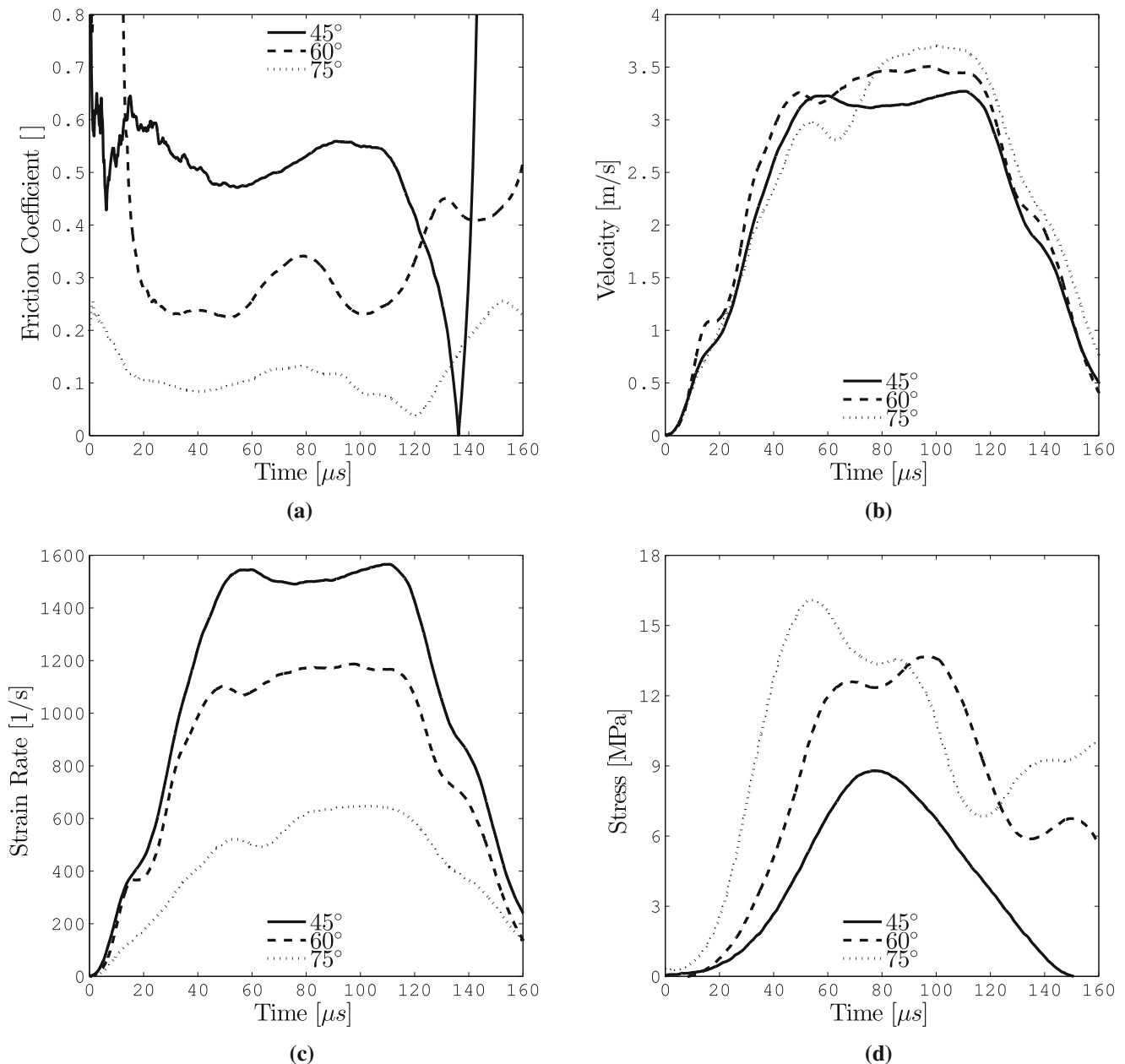


Fig. 8 Dynamic friction experiments. **(a)** The friction coefficient produced with the three torque adapters. The initial and final sections are poorly defined due to the small compression stress. As the compression increases, the friction becomes more consistent. **(b)** The resulting sliding velocity produced by the three torque adapters. The increase in angle of inclination produces an increase, although not significant, in sliding velocity, a quantity directly proportional to the angular velocity of the torque adapter. **(c)** The axial strain rate seen by the specimen in the friction experiments. Most of the kinetic energy is converted to rotational motion, resulting in less axial motion of the torque adapter with higher inclination angles. **(d)** The axial compression stress of the specimen. This is the response of the specimen with dynamic compression and friction loading

by the length of the striker and its bar wave speed), a factor which was not considered in this study. Limitations from the modifications are imposed by the geometry of the torque adapter itself, requiring only small angle changes to reduce the complexity of data reduction. This limitation is possible to overcome if a true screw or a double helix with sufficient tolerances can be achieved.

Lastly, care must be taken in the experiments to ensure that the torque adapter has not closed during the loading period(s). Since the relation between the resulting compression and shear is only dependent on the slope of the contact between the two mating pieces of the torque adapter, and not on the relative angle, the data reduction will still produce a non-zero angular velocity even though it is

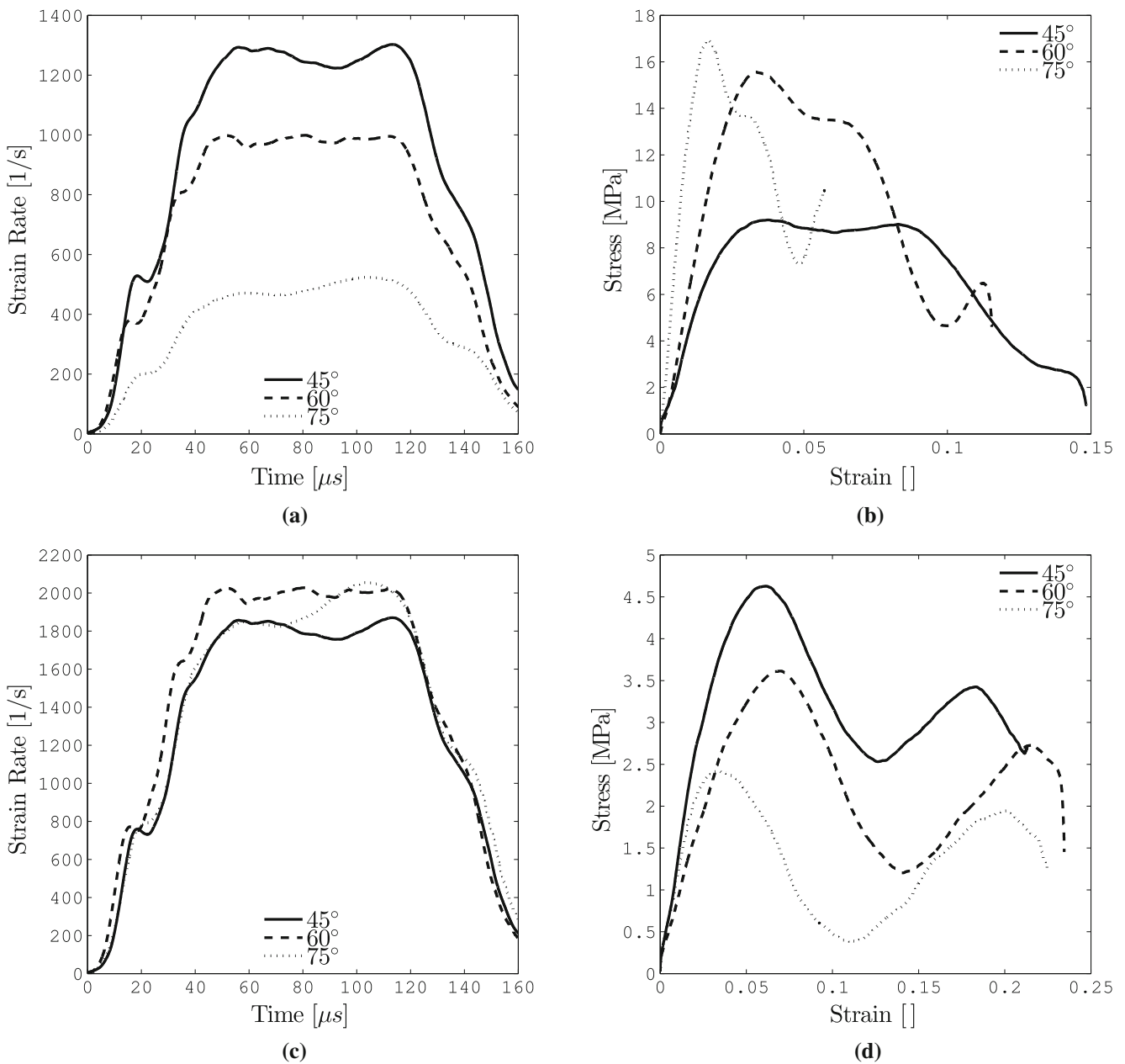


Fig. 9 Compression-shear experiments. **(a)** The axial strain rate seen by the specimen in the shear experiments. The same trend is apparent as in the friction experiments, a result of the geometry of the torque adapter. **(b)** The axial stress-strain response of the specimen. Increased angle of inclination produces lower strain rates and hence lower total strain. **(c)** The shear strain rate seen by the specimen in the shear experiments. The response of the specimen is more important in the shear experiments, thus reducing the shear strain rate produced by the torque adapter. **(d)** The shear stress-strain response of the specimen. Unlike compression, the total shear strain is determined by the total angle of twist, which is in turn determined by the forward motion of the incident bar, a quantity which was kept constant for all of the experiments

physically impossible for the torque adapter to be rotating any further.

Initial Angle

Because of the nature of the inclined plane on a circular cross-section, the path of the contact point is elliptical. This means that the axial and rotational components vary not

only with the pitch angle (θ), but also with the ordinate angle (ϕ) (Fig. 10). The assumption that the torque adapter does not close is sufficient for a short incident wave, where deviation from the initial angle of the torque adapter is small (Fig. 10). For experiments requiring large strains or longer loading periods, a torque adapter featuring a true screw or double helix would be preferable to avoid the implications of this assumption and the effects of the inclined planes.

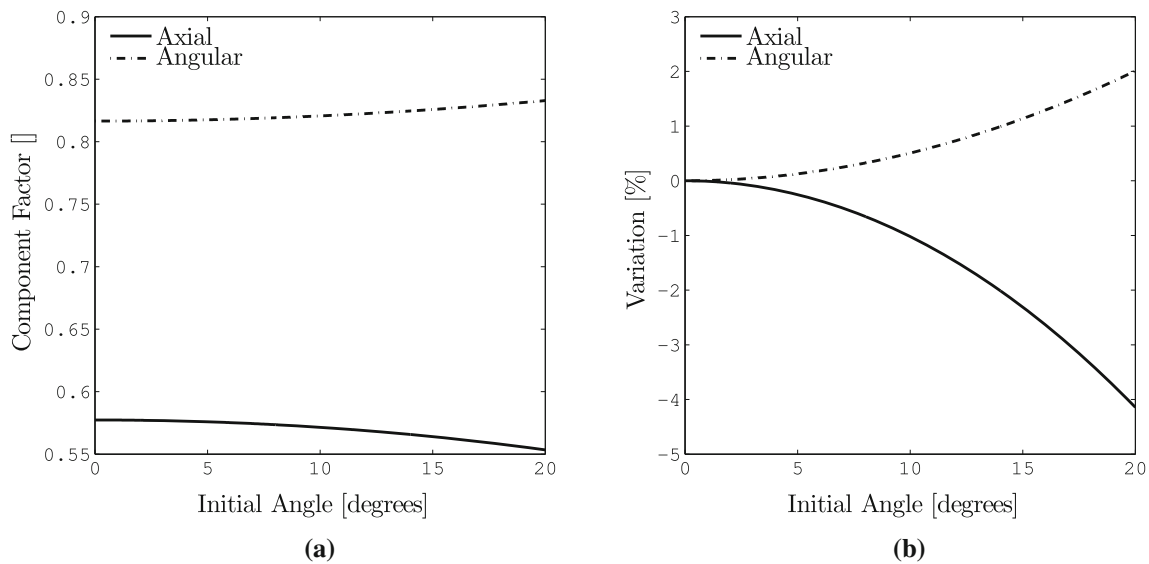


Fig. 10 Characteristics of torque adapter geometry. **(a)** Factors relating the bar end velocity to the axial and rotational motion of the torque adapter for inclined planes of 45 degrees. Deviation from the central contact point (when the angle is zero) produces stronger rotational effects because of the decreasing pitch on the elliptical path. **(b)** Variation of the component factors in percent for inclined planes of 45 degrees. For short loading durations, the angle of the torque adapter will not change significantly, and does not need to be accounted for during data reduction. Higher angles of inclination have smaller variations in the two factors

Verification of Contact

The length of the torque adapter plays a subtle role in the dynamics of the system. Due to the effects of wave propagation, the adapter could experience much higher angular velocities than the incident bar. Without a specimen and set of transducers (or transmission bar), the adapter would separate from the incident bar in the axial direction. With a specimen in place, the likelihood of separation becomes very small. However, if the torsional stiffness of the specimen is very small, the small resultant torque on the adapter might not be sufficient to keep the inclined planes (or screw) fully mated throughout the duration of the experiment, as the reflection of torsional waves within the adapter would allow premature separation.

In addition, the set of sliding inclined planes within the torque adapter is also affected by friction. Since the torque adapter exists prior to the specimen (in terms of wave propagation), this frictional quantity does not affect the loading measurements, which are measured directly by the force and torque transducers. Rather, the target loading rates (axial strain rate, shear strain rate, and sliding velocity) may be directly impacted for non-negligible friction in the torque adapter.

The most straight forward method to verify the motion of the torque adapter is through the use of a high speed camera (Fig. 11). Even though the adapter experiences a high angular velocity, the short duration of the incident pulse results in only a small change in the angle. Furthermore, the imagery

confirms that the data reduction is correct in determination of the angular velocity, forward velocity, and opening angle.

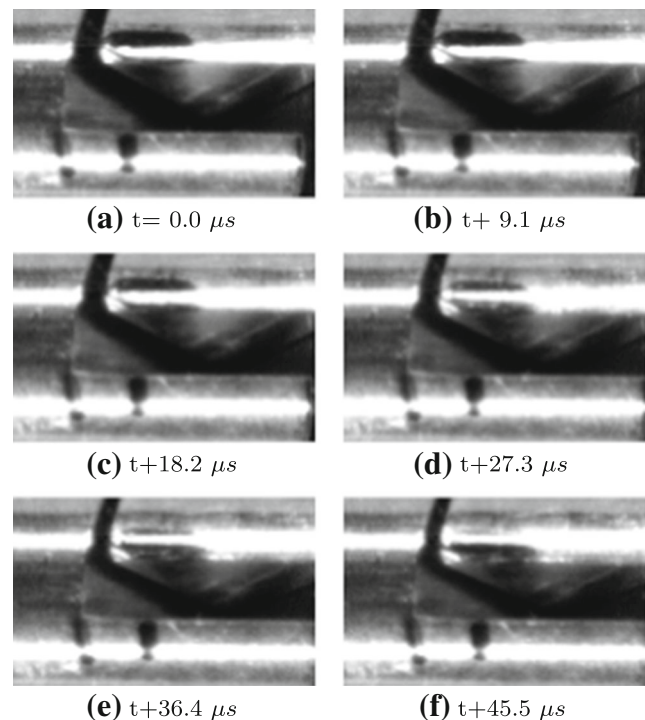


Fig. 11 Six high speed images at various points through the motion of the torque adapter during the first incident pulse. The images are useful for verifying both the angle and angular velocity as a function of time

Load Transducers

The dynamic nature of the Kolsky bar experiment restricts the use of load transducers because of the large accelerations involved. While axial force transducers can be found in small sizes and high sensitivities, torque sensors cannot. The reasoning behind this is that torque sensors typically require an axial compressive preloading, resulting in a relatively larger transducer compared to a transducer meant for measuring axial forces. The effects of a large transducer come in two forms: a delay for traversal of the torsional wave, and smoothing of the profile due to inertia. In principal, the small loads expected from the experiments should not present sufficiently high accelerations to induce inertial effects. However, the length of the transducer assembly could produce a delay in signal measurement of up to 20 micro-seconds. This delay should be calibrated for the transducer in use and must be included in the data reduction process when selecting the compressive and torsional measurements.

The transducer assembly in the study consisted of two individual transducers coupled together. The coupling was accomplished through an alignment plate that was capable of being fastened to both the force and torque transducers. The torque transducer had multiple mounting holes, optimal for transmitting torque, but the force transducer had one central threaded hole. In order to reduce the effects of the thread, the torque adapters were designed to provide a torque that would tighten the force transducer to the torque transducer. Considering that the applied torques were also small, securely mounting the force transducer with an even greater torque effectively removes concerns regarding slip and rotation of the force transducer during an experiment. Furthermore, since the loads are fairly small due to the softness of the material (PBXn-301 simulant), error due to load coupling in the force transducer and the torque transducer were considered to be negligible.

Conclusion

The compression Kolsky bar was modified to dynamically load a specimen in compression and torsion simultaneously. The technique is applicable to both dynamic friction experiments and shear stress-strain experiments. The study was limited to soft materials, and used a set of transducers instead of a transmission bar, but the technique is applicable to the study of hard materials as well, and may be used with a transmission bar. Experiments show that increasing the pitch of the torque adapter produces equivalent increases in rotational motion (either shear strain or sliding velocity). The simultaneous application of compression and shear

enables the characterization of materials and verification of material models in multi-axial states of stress.

Acknowledgements This research was supported by a cooperative agreement between Air Force Research Laboratory and Purdue University (FA8651-13-2-0005). We also acknowledge for the inspiration from Dr. Dan Casem of Army Research Laboratory in the design and application of this experimental technique.

References

1. Chen WW, Song B (2010) Split Hopkinson (Kolsky) bar: design, testing and applications. Springer Science & Business Media
2. Kolsky H (1949) An investigation of the mechanical properties of materials at very high rates of loading. *Proc Phys Soc Sect B* 62(11):676
3. Christensen R, Swanson S, Brown W (1972) Split-hopkinson-bar tests on rock under confining pressure. *Exp Mech* 12(11):508–513
4. Frew DJ, Akers SA, Chen W, Green ML (2010) Development of a dynamic triaxial kolsky bar. *Meas Sci Technol* 21(10):105–704
5. Duffy J, Campbell J, Hawley R (1971) On the use of a torsional split hopkinson bar to study rate effects in 1100-0 aluminum. *J Appl Mech* 38(1):83–91
6. Nemat-Nasser S, Isaacs JB, Starrett JE (1991) Hopkinson techniques for dynamic recovery experiments. *Proc R Soc Lond A Math Phys Sci* 435(1894):371–391
7. Baker WE, Yew C (1966) Strain-rate effects in the propagation of torsional plastic waves. *J Appl Mech* 33(4):917–923
8. Espinosa H, Patanella A, Fischer M (2000) A novel dynamic friction experiment using a modified kolsky bar apparatus. *Exp Mech* 40(2):138–153
9. Rajagopalan S, Prakash V (1999) A modified torsional kolsky bar for investigating dynamic friction. *Exp Mech* 39(4):295–303
10. Claus B, Nie X, Martin B, Chen W (2015) A side-impact torsion kolsky bar. *Exp Mech*, pp. 1–8
11. Nie X, Prabhu R, Chen W, Caruthers JM, Weerasooriya T (2011) A kolsky torsion bar technique for characterization of dynamic shear response of soft materials. *Exp Mech* 51(9):1527–1534
12. Ogawa K (1997) Impact friction test method by applying stress wave. *Exp Mech* 37(4):398–402
13. Huang H, Feng R (2004) A study of the dynamic tribological response of closed fracture surface pairs by kolsky-bar compression-shear experiment. *Int J Solids Struct* 41(11):2821–2835
14. Huang H, Feng R (2007) Dynamic friction of sic surfaces: a torsional kolsky bar tribometer study. *Tribol Lett* 27(3):329–338
15. Lewis JL, Goldsmith W (1973) A biaxial split hopkinson bar for simultaneous torsion and compression. *Rev Sci Instrum* 44(7):811–813
16. Rittel D, Lee S, Ravichandran G (2002) A shear-compression specimen for large strain testing. *Exp Mech* 42(1):58–64
17. Zhao J, Knauss W, Ravichandran G (2009) A new shear-compression-specimen for determining quasistatic and dynamic polymer properties. *Exp Mech* 49(3):427
18. Zhao P, Lu F, Chen R, Lin Y, Li J, Lu L, Sun G (2011) A technique for combined dynamic compression-shear test. *Rev Sci Instrum* 82(3):035–110
19. Lin Y, Qin J, Lu F, Chen R, Li X (2014) Dynamic friction coefficient of two plastics against aluminum under impact loading. *Tribol Int* 79:26–31

